Estrogen Depletion Results in Nanoscale Morphology Changes in Dermal Collagen

Ming Fang[1,2], Kaitlin G. Liroff[1], A. Simon Turner[3], Clifford M. Les[3,4], Bradford G. Orr[2,5,6] and Mark M. Banaszak Holl[1,2,6]

Tissue cryo-sectioning combined with atomic force microscopy imaging reveals that the nanoscale morphology of dermal collagen fibrils, quantified using the metric of D-periodic spacing, changes under the condition of estrogen depletion. Specifically, a new subpopulation of fibrils with D-spacings in the region between 56 and 59 nm is present 2 years following ovariectomy in ovine dermal samples. In addition, the overall width of the distribution, both values above and below the mean, was found to be increased. The change in width due to an increase in lower values of D-spacings was previously reported for ovine bone; however, this report demonstrates that the effect is also present in non-mineralized collagen fibrils. A nonparametric Kolmogorov–Smirnov test of the cumulative density function indicates a statistical difference in the sham and OVX D-spacing distributions ($P<0.01$).

Journal of Investigative Dermatology (2012) **132,** 1791–1797; doi:10.1038/jid.2012.47; published online 22 March 2012

INTRODUCTION

The dermis layer of skin is primarily composed of type I collagen fibers (85–90%), elastic fibers, and glycosaminoproteoglycans (Castelo-Branco *et al.*, 1993). Collagen fibrils account for skin's tensile strength and resilience, whereas the elastic fibers contribute to the elasticity and extensibility of skin (Goldsmith, 1991). Unlike collagen in bone, which is frequently remodeled to maintain its mechanical strength, skin collagen has a remarkably long half-life under normal conditions (Verzijl *et al.*, 2000), and thus suffers long-term degradation due to skin aging. The severity of skin aging differs by the anatomical locations: sun-protected skin suffers from mainly intrinsic aging effects associated with time, such as fine wrinkles and reduced elasticity, whereas sun-exposed skin suffers both intrinsic and extrinsic aging (exposure to external influences such as UV radiation), where the severity and rate of the pathological changes including deep wrinkles, pigmentation, and melanoma formation, are exacerbated (Bolognia, 1995; Gilchrest, 1996; El-Domyati *et al.*, 2002; Naylor *et al.*, 2011). The process of skin aging leads to decreased skin collagen content, moisture, and elasticity (Uitto, 1986; Brincat *et al.*, 1987). A recent study has shown that collagen fibrils are fragmented in aged human skin. These changes in the extracellular environment affect fibroblast attachment and production of matrix metalloproteinases, which in turn accelerates extracellular matrix degradation (Fisher *et al.*, 2009). This work underscores the importance of characterizing collagen in order to better understand the effects of aging on skin.

Estrogen has many beneficial and protective effects on skin physiology and functions, including maintenance of hydration and skin thickness, wound healing, and reduction of skin cancer risk (Brincat, 2000). At the molecular level, estrogen exerts its effect by interacting with surface or intracellular estrogen receptors. Intracellular estrogen receptors, ER-α and ER-β, have been identified in dermal fibroblasts (Haczynski *et al.*, 2002). The cellular responses triggered by the level of estrogen involve gene transcription/expression, as well as cytoplasmic signaling pathways. At the macroscopic level, aging, and especially the onset of menopause, causes a series of deteriorations in skin tissue physiology as a consequence of compositional and structural alterations in the extracellular matrix proteins. Postmenopausal women suffer from loss of dermal collagen content at an average rate of 2% per postmenopausal year over a period of 15 years (Brincat *et al.*, 1983, 1985, 1987, 2005). Decreased amounts of elastic fibers and glycosaminoproteoglycans in postmenopausal years lead to compromised skin elasticity and less binding with water, respectively (Uitto, 1986; Waller and Maibach, 2006; Sherratt, 2009). The thinning of the dermal layer and loss of water gradually result in wrinkle formation. At the microscopic level, little is known about the ultrastructural changes of dermal proteins that accompany aging and menopause. In this study, we examined the effect of estrogen depletion on the nanoscale morphology of collagen fibrils in ovine dermis. We used the metric of fibril D-spacing, which captures a number of

[1]*Department of Chemistry, University of Michigan, Ann Arbor, Michigan, USA;* [2]*Michigan Nanotechnology Institute for Medicine and Biological Science, University of Michigan, Ann Arbor, Michigan, USA;* [3]*College of Veterinary Medicine and Biomedical Sciences, Colorado State University, Fort Collins, Colorado, USA;* [4]*Bone and Joint Center, Henry Ford Hospital, Detroit, Michigan, USA;* [5]*Department of Physics, University of Michigan, Ann Arbor, Michigan, USA and* [6]*Program in Applied Physics, University of Michigan, Ann Arbor, Michigan, USA*

Correspondence: Mark M. Banaszak Holl, Department of Chemistry, University of Michigan, 930 N. University Avenue, Ann Arbor, Michigan 48109-1055, USA. E-mail: mbanasza@umich.edu

Abbreviation: AFM, atomic force microscopy

Received 8 June 2011; revised 23 October 2011; accepted 29 October 2011; published online 22 March 2012

structural features, including the molecular structure of the collagen, the three-dimensional fibril formation, and the associated post-translational modifications.

Studies indicating that the D-spacing in collagen exists as a distribution of values ranging from about 64 to 73 nm were recently reported for murine bone, dentin, and tendon tissue (Wallace *et al.*, 2010a). The importance of using a technique that measures the fibril D-spacing on a fibril-by-fibril basis, as opposed to X-ray or optical methods, which average over micron to millimeter scales when obtaining D-spacing data, was highlighted by studies examining the effect of genetic changes, *Osteogenesis Imperfecta*, or estrogen depletion upon the D-spacing distribution in bone tissue (Wallace *et al.*, 2010b, 2011). In both cases, the average D-spacing values did not change significantly, but the distributions of D-spacings were significantly different.

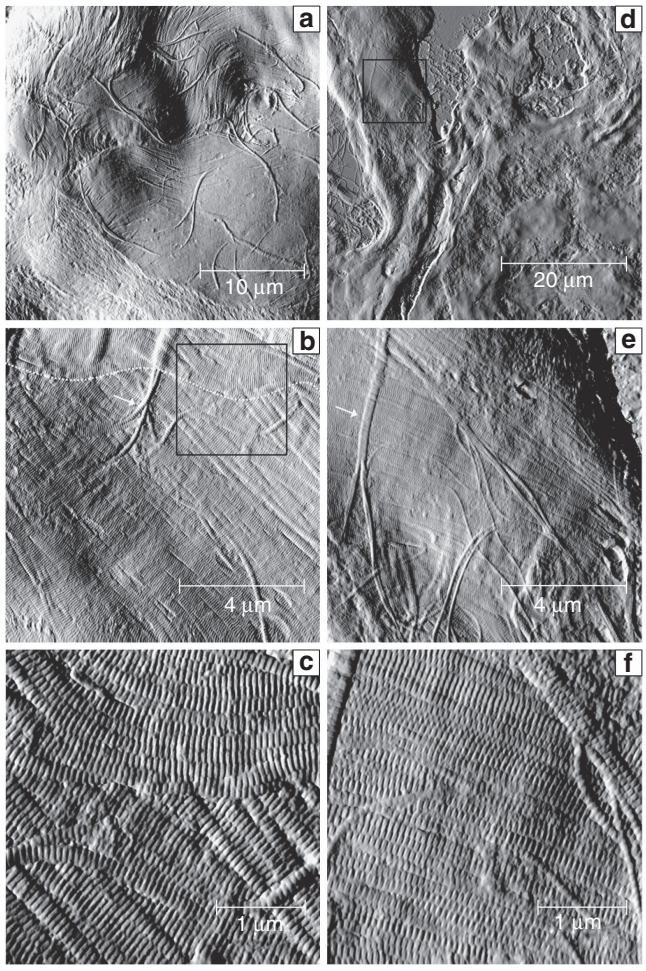

Figure 1. Atomic force microscopy deflection images of ovine dermis contain domains of collagen fibril bundles. (**a**–**c**) Representative images from a sham dermis sample; (**d**–**f**) images from an ovariectomy (OVX) dermis sample. Panel **a** captures potentially two fibril bundles (the rough area at the bottom of the scan is caused by microtome sectioning). Panel **b** shows one fibril bundle on top of another (the boundary is marked by the white dashed line); note that a few fibrils (see the white arrow) that are underneath one bundle are on the surface of another bundle. Panel **c** is the region marked by the black box in panel **b**. Panels (**e**) and (**f**) capture the only region with collagen fibrils found in the 50-micron area of OVX dermis (panel **d**).

Long-term ovariectomy (OVX) in ovine leads to compromised compact bone viscoelastic properties, which are similar to the conditions in postmenopausal women (Les *et al.*, 2005). Mineralization, architecture, and remodeling parameters of OVX ovine bones have been characterized, and intriguingly only poor correlation between viscoelastic mechanical properties and these parameters were found (Les *et al.*, 2004). Additional quality factors that come from non-mineral components of bone are speculated to have a crucial role in decreasing bone viscoelastic properties. Similar biochemical and biomechanical effects have been noted between estrogen-deprived skin and bone (Pierard *et al.*, 1995, 2001; Ozyazgan *et al.*, 2002). We are interested in characterizing the fibrillar collagen D-spacing in hope of better understanding the mechanisms of mechanical failure in ovariectomized tissue. D-spacing has been demonstrated as an effective evaluation of fibril strain in bone and tendon previously. Mechanical stretching at the tissue level can lead to increased fibril level strain, and therefore increased D-spacings (Gupta and Zioupos, 2008; Gupta *et al.*, 2010). Atomic force microscopy (AFM) imaging of the ultrastructure of type I collagen provides a means to probe the integrity of the matrix protein and its association with macroscopic pathologies. Previously, we have found a marked difference in the D-spacing population distribution between sham control and OVX ovine cortical bone, suggesting that long-term estrogen deprivation leads to a decrease in fibril D-spacing (Wallace *et al.*, 2010b).

In this study, we quantified the D-spacing distribution present in ovine skin and examined the effect of estrogen depletion upon the distribution. It was shown that collagen in skin also exhibits a distribution of D-spacing values, as opposed to the singular value of ~67 nm for tendon and bone or 65 nm for skin, typically discussed in textbooks and reviews, and that this distribution changes upon estrogen depletion. This study demonstrates that the distribution of D-spacings is independent of the degree of tissue mineralization. It is particularly interesting to note that estrogen depletion causes similar changes in the nanoscale morphology of fibrils in both skin and bone.

RESULTS

The combination of cryostat sectioning and AFM imaging has been recently highlighted by Graham *et al.* (2010) as an advantageous tool for morphological studies of collagen matrix protein structures in soft tissues. Although histological data reveal the orientation and organization of collagen fibril bundles in the dermis, the resolution is limited in resolving fibril organizations within a bundle. AFM imaging can overcome this issue, and representative images of fibril bundles from ovine dermis are illustrated in Figure 1. Qualitatively, on the 50-micron scale and above, the fibril bundles were randomly oriented in a wavy pattern; within a fibril bundle, on the order of 10-micron scale, collagen fibrils were bundled in a parallel longitudinal direction and individual fibrils crossing the bundle domains were frequently observed (see the arrowheads in Figure 1b and e). The function of these crossing fibrils is unclear.

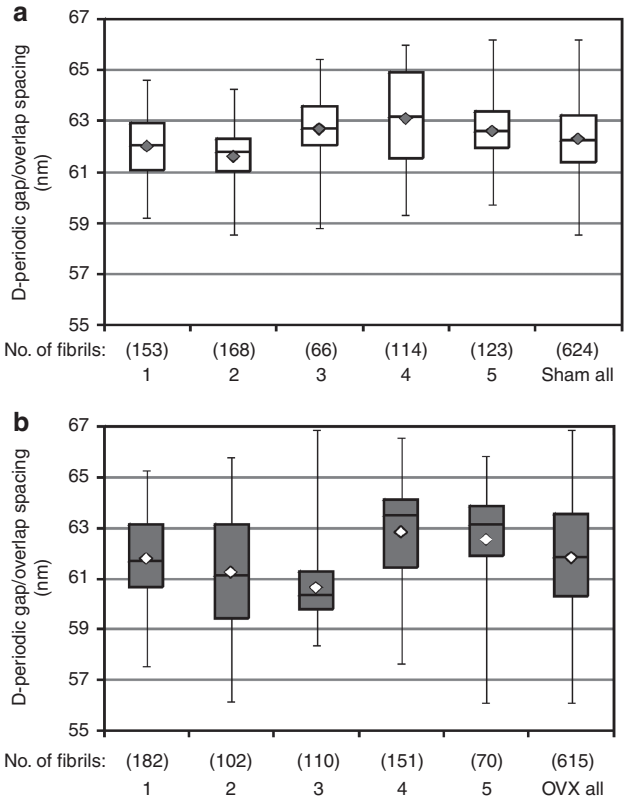

Figure 2. Box plot representation of D-periodic spacing from sham and ovariectomy (OVX) ovine dermis. D-periodic gap/overlap spacings from (**a**) individual sham ($n=5$) and (**b**) OVX ($n=5$) ovine dermis. The box plot shows the interquartile (middle 50% of data), the horizontal line inside the box is the mean, the diamond is the median, and the whiskers denote the minimum and maximum observations. The numbers in parentheses are numbers of fibrils measured in each specimen. Two-tailed Student's *t*-tests between the sham and OVX group suggest no differences between the means ($P=0.249$).

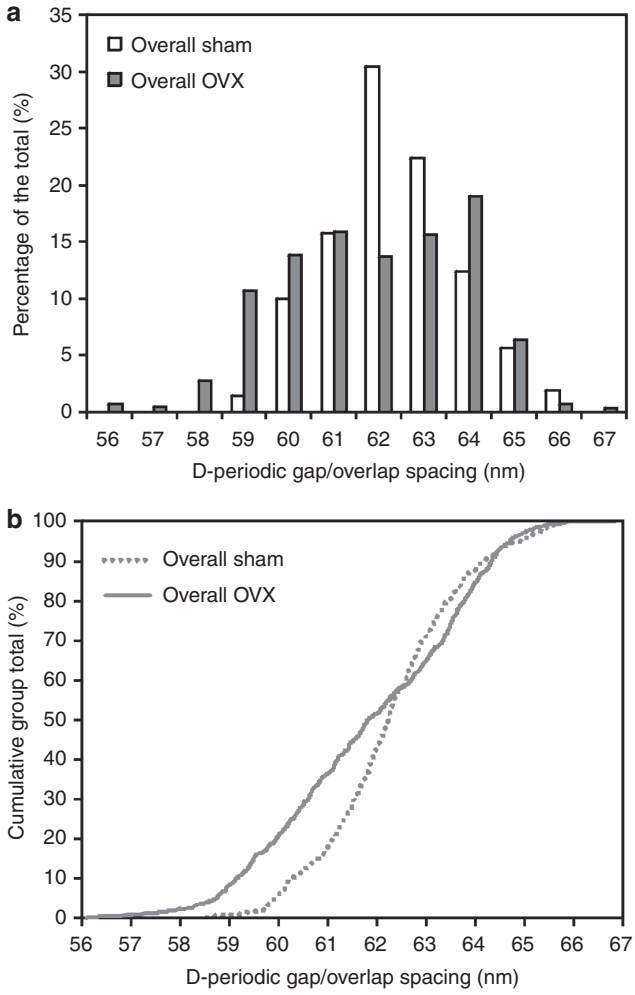

Figure 3. Histogram and cumulative distribution function of D-periodic spacings from the sham and OVX ovine dermis (each contains five animals). (**a**) Histogram representation of D-periodic gap/overlap spacings from the sham and OVX ovine skin (1-nm bin size). (**b**) The cumulative distribution function calculated from each group. A Kolmogorov–Smirnov test performed on the data distributions indicates significant difference ($P<0.001$).

Quantitatively, the characteristic collagen fibril D-spacing was measured and used as the main morphological metric. For each biopsy, at least 60 fibrils from a minimum of four and an average of five randomly selected 50-micron locations were analyzed. The difference in the number of fibrils obtained for each biopsy is due to variation in collagen abundance at the location of AFM tip engagement. Measurements from each skin biopsy were pooled together to yield the average D-spacing (Figure 2). The mean values for five sham ovine were 62.0, 61.6, 62.7, 63.1, and 62.6 nm. The mean values for the OVX ovine were 61.8, 61.3, 60.7, and 62.5 nm. The means from sham and OVX were not significantly different ($P=0.249$) when compared with the two-tailed Student's *t*-test.

Examination of the population histogram (Figure 3a) revealed that the sham D-spacing distribution spans between 59 and 66 nm, whereas the OVX population spans between 56 and 67 nm. The major difference between these populations arises from the percentage of fibrils with D-spacings from 56 to 59 nm—14.6% in the OVX group and 1.6% in the sham group. Note that these changes in distribution did not have a significant impact on the mean D-spacing values, which were 61.9 nm for the OVX and 62.3 nm for the sham specimens. The distributions were not strictly Gaussian and the OVX distribution in particular appeared bimodal, making the use of the mean value statistically incorrect. We provided it here so that a rough comparison with previous literature could be made; however, to correctly analyze the data, a nonparametric method must be used.

To determine the statistical significance of these distributions, a cumulative density function was plotted and evaluated using the nonparametric Kolmogorov–Smirnov test (Figure 3b). The cumulative density function highlights the cumulative difference in the 56–62 nm region, and the distributions were found to be significantly different ($P<0.001$).

Depending on species and tissue type, mature collagen fibril diameter varies markedly. In developed ovine dermis, collagen fibril diameter is about 100 nm (Flint *et al.*, 1984). To evaluate the effect of estrogen depletion, fibril diameters were measured by averaging the fibril bundle width. The results indicated that OVX ovine dermis has a fibril diameter

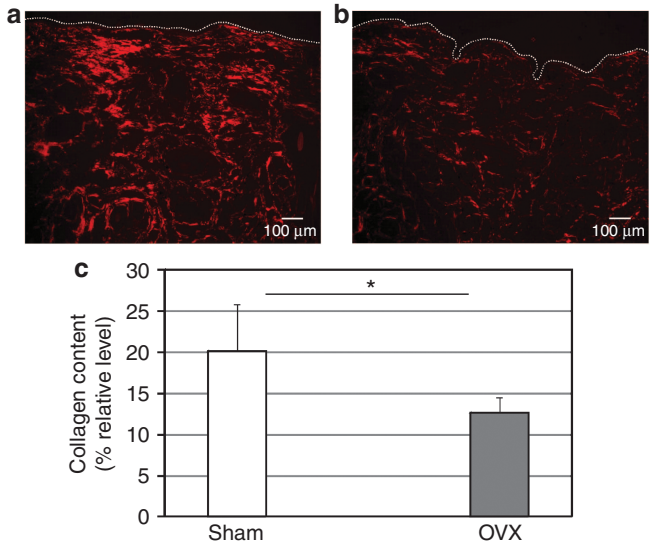

Figure 4. Sirius red staining reveals the abundance of fibrillar collagen content in sham and ovariectomy (OVX) dermis. (**a**, **b**) Polarized light-microscopic images of sham and OVX dermis, respectively. Orginal magnification × 10. Dashed lines represent the epidermis. (**c**) Collagen abundance measured from the staining intensity (*$P<0.05$).

similar to that of sham ovine. In the case of sham ovine, fibril diameter ranges from 80 to 180 nm, with an average of 130 ± 30 nm. OVX ranges from 80 to 160 nm and has an average of 120 ± 20 nm. In collective tissues, fibril diameters are typically assessed in the cross-sectional plane; diameter measurements in the axial plane are limited in accuracy because fibril overlapping is inevitable in tissue sections. Averaging from parallel bundles remedies this problem to a certain degree and ensures ± 10 nm accuracy (for more details see the Supplementary Information online).

To explore the effect of estrogen on collagen content in ovine dermal skin, we performed Sirius red staining followed by polarized light-microscopic imaging. Because the birefringence is highly specific to fibrillar collagen owing to its uniaxial anisotropy (Cuttle *et al.*, 2005; Junqueira *et al.*, 1978), the staining serves as a good indication of collagen fibril abundance. Figure 4 indicates higher abundance of fibrillar collagen in sham dermis ($P<0.05$) and a qualitatively thicker fibril bundle width than in OVX dermis.

DISCUSSION

AFM is a nondestructive alternative for imaging biological tissues under aqueous conditions; however, imaging bulk skin tissue using AFM can be challenging because collagen fibril bundles are surrounded by a sol–gel of hydrophilic glycosaminoproteoglycans and subcutaneous adipose fat. Recently, Graham *et al.* (2010) reported a combined tissue cryosectioning and AFM imaging method that provided excellent resolution of the ECM components in skin, cartilage, aorta, and lung. The sample preparation greatly facilitates AFM imaging and characterization of biological tissues while avoiding fixation, chemical staining, and high vacuum.

To evaluate the nanomorphology of collagen fibrils present in the dermis, we selected the D-spacing as a reliable quantitative marker. We have previously demonstrated that the application of two-dimensional fast Fourier Transforms allows an accurate evaluation of this prominent fibril feature. The D-spacing arises from a parallel staggered packing of collagen monomers, which lead to alternating gap and overlap zones along the longitudinal axis of a fibril, as illustrated by the two-dimensional Hodge–Petruska model (Hodge and Petruska, 1963). A recent X-ray crystallographic work by Orgel *et al.*, (2001) provides additional three-dimensional insight, which supports a supertwist microfibril model. These structural models indicate that quantitative analysis of the D-spacing should be sensitive to changes in the collagen molecule triple helix, the molecular packing, and intermolecular cross-linking effects. For example, the single amino-acid substitution of a cysteine residue for glycine-349 results in nanoscale morphology changes observed in the collagen fibril D-spacing distribution. Moreover, the free-energy changes induced by amino acid substitution correlate with clinical severity of *Osteogenis Imperfecta* (Lee *et al.*, 2011).

Quantitative analysis of ovine dermis collagen D-spacings indicates a distribution of values is present ranging from 56 to 67 nm with a mean value of 62 nm. Although AFM has an excellent ability to differentiate differences in the D-spacing within tissue, the absolute value is limited by the calibration process. The average value of the distribution of 62 nm was close to previous literature values obtained by X-ray scattering. Purslow *et al.* (1998) reported 67-nm D-spacing in rat skin; others reported lower values of about 65 nm for skin (Brodsky *et al.*, 1980; Stinson and Sweeny, 1980; Gathercole *et al.*, 1987). These techniques have spot sizes of microns, and thus average over too large an area of the skin structure for observation of a D-spacing distribution. The observation of this distribution in dermal collagen provides further evidence that distribution of values is an intrinsic aspect of collagen fibrillar structure. A similar distribution has previously been observed for another non-mineralized type 1 collagen tissue, murine tail tendon, as well as for the mineralized collagen tissues murine dentin and bone and ovine bone (Wallace *et al.*, 2010a, b, 2011). The observation of the distribution was possible because of the fibril-by-fibril analysis using the AFM data.

The influence of bulk tissue stress on collagen fibril D-spacings has been the subject of numerous studies. Gupta and Zioupos (2008) demonstrated a connection between fibril stain and D-spacing. They noted a 0.3-nm increase in D-spacing in bone as measured by small-angle X-ray scattering under mechanical stretching. For bone, fibril strain accounts for only a fraction of the total tissue strain, suggesting that interfibrillar sliding and shear of the proteoglycan-rich matrix takes up the remainder of the tissue strain. With regard to tendon, Puxkandl *et al.* (2002) demonstrated up to a 1-nm change when a 3% macroscopic strain was used and a 0.2-nm change at a 1% strain. D-spacing changes varied between 0.2 and 2 nm at tendon fracture. The most general conclusion from the comparison of these data with the distribution of D-spacings that we report, which has a width of 12 nm, was that materials' strain effects on

D-spacing are not large enough to explain the D-spacing distribution observed in either mineralized or non-mineralized biological tissues. The strain effects tend to be about an order of magnitude too small.

One limitation of the current study was that we used dorsal skin exposed to UV radiation as opposed to skin protected from extrinsic UV radiation. Ovine dermis is considerably thicker than human dermis (Dellmann and Eurell, 1998); in addition, a layer of wool equivalent to sun protection factor 30 also makes it difficult to assess how much photoaging is induced in these dermal tissue samples as compared with human samples (Forrest and Fleet, 1986; Fleet, 2006). However, given that the sham and OVX ovine were provided with the same sheltering condition, the effects observed in this study signify change in the hormonal level rather than differential UV radiation exposure.

Estrogen is known to have important roles in mediating connective tissue physiology and function. Estrogen depletion associated with menopause causes detrimental effects on the connective tissues. In skin, estrogen depletion is associated with declining dermal collagen content, skin thickness, water-holding capacity, and skin elasticity. In terms of mechanical properties, a steep increase in skin extensibility was noted in women during perimenopause (Pierard *et al.*, 1995), and ovariectomized rats exhibit an increased Young's Modulus in the skin (Ozyazgan *et al.*, 2002). Reduced estrogen level also impairs the rate and quality of wound healing: in postmenopausal women and in ovariectomized female rodents, a marked delay in wound healing was reported (Ashcroft *et al.*, 1997; Calvin *et al.*, 1998). Hormone replacement therapy was found to partially reverse these effects, and topical application of estrogen on wounded skin accelerated wound healing (Ashcroft *et al.*, 1999). In addition, Pierard and co-workers noted a positive correlation between bone mineral density and skin viscoelasticity in women (Pierard *et al.*, 2001).

Collagen ultrastructure in ovine bone demonstrated significant change with estrogen depletion; 28% of fibrils in OVX ovine have D-spacings lower than 64 nm, whereas sham-operated ovine contained 7% of such fibrils with low D-spacings (Wallace *et al.*, 2010b). The results presented here show that similar changes occur in dermal collagen nanomorphology upon estrogen depletion. Although the percentage of low D-spacing fibrils (less than 59 nm) was lower in the dermis, 14.6% in the OVX group, and 1.6% in the sham group, the result was persistent in all the five OVX animals we examined. Bone is a mineralized connective tissue, whereas dermis is only constituted of macromolecular proteins. Thus, the results indicate that the changes in collagen nanomorphology result from changes in the protein structure, most likely post-translational modifications, and/or the structural interactions with other tissue proteins such as decorin (Danielson *et al.*, 1997), and is not a mineralization-related structural change.

Fibril diameter has been used previously as a key measure of ultrastructural change. A number of diseases and tissue malfunctions are associated with changes in collagen fibril diameter. Decorin and lumican knockout rats and type V collagen–deficient mice showed 1-fold increase in fibril diameters (Wenstrup *et al.*, 2004; Yeh *et al.*, 2010). Ovarectomy has been shown to decrease expression level of proteoglycans, including decorin (Danielson *et al.*, 1997) and lumican (Markiewicz *et al.*, 2007). In this study, the average collagen fibril diameter in sham was about 130 ± 30 and 120 ± 20 nm in OVX; the difference was less than 10% and considered negligible given the limited accuracy in the analysis. Thus, estrogen depletion exerts an anisotropic effect on skin collagen's ultrastructure. It is unclear whether decorin and lumican deficiency are associated with collagen fibril D-spacing changes; this will be the subject of future studies.

In conclusion, estrogen depletion causes a change in the nanoscale morphology of dermal collagen, quantitatively demonstrated by change in the D-spacing metric. The morphology changes are similar to those previously observed for bone collagen, suggesting that estrogen depletion acts upon a structural aspect of the collagen molecule and/or associated proteins and are intrinsic to the fibril formation process.

MATERIALS AND METHODS

Animals

Six-year-old Columbia-Rambouilliet cross ovine were anesthetized and ovariectomized (OVX, $n = 5$); the control group was subjected to a sham surgery (sham, $n = 5$; Colorado State University, ACUC #03-010A-02) as part of a larger study. Two years after the surgery, the animals were killed with an intravenous overdose of a barbiturate, and skin specimens were procured on the dorsal thoracolumbar region centered at the midline, a region that is subject to both intrinsic and extrinsic aging. Specimens were wrapped in saline-soaked towels, placed in a plastic zip-lock bag, and frozen at $-20\,^{\circ}C$.

Cryostat sectioning

First, 1 cm × 1 cm skin specimens were cut and subcutaneous fat layer was removed using a scalpel blade. Samples were then embedded in Tissue-Tek optimal cutting temperature solution (Sakura Finetek, Torrance, CA) and frozen at $-20\,^{\circ}C$. Thin sections (10-μm-thick) of skin were obtained using Mithcrom HM550 Cryostat (Thermo Scientific Walldorf, Germany) and transferred onto glass slides. The dermal sections were rinsed with ultrapure water for 5 min and kept at $-20\,^{\circ}C$ before the AFM study on the next day. The combined cryo-section and AFM imaging was described in a recent report by Graham *et al.* (2010).

AFM imaging and analysis

The AFM imaging on OVX and sham dermal sections was carried out in air using a PicoPlus 5500 AFM (Agilent, Santa Clara, CA), in contact mode with SNL-10 AFM probes (Bruker AFM probes, nominal tip radius 2 nm, force constant 0.25 $N\,m^{-1}$). The set point and gains were optimized in each scan to maintain a minimum level of tip–sample contact and no lateral dragging was observed in the images. Line-scan rates were set at 2 Hz or lower at 512 lines per frame. Measurements were recorded and image analysis was performed using the SPIP software (V 5.0.8, Image Metrology, Horsholm, Denmark). Collagen fibril D-spacings were measured using the two-dimensional fast Fourier transform (FFT) toolkit of the SPIP software; detailed description and validation can be found in previous studies (and the Supplementary Information online;

Wallace *et al*., 2010b). In short, a straight fibril with at least nine D bands was selected and marked by a rectangular box as the region of interest; the two-dimensional fast Fourier Transforms were carried out on the region of interest, and the periodic information (i.e., D-spacing) was obtained from the FFT image. This method provides measurements with an uncertainty of 0.8 nm, therefore the bin size in the population histogram was set to 1 nm.

Statistical analysis of AFM data

Statistical analyses used PASW (Version 18, SPSS). A P value less than 0.05 was considered significant for all analyses. The mean D-spacing values for all sham ovine ($n=5$) and OVX ovine ($n=5$) were compared using the two-tailed Student's t-test. To examine differences in the population distribution of fibril nanomorphology between sham and OVX groups, the cumulative distribution function of each group was calculated and Kolmogorov–Smirnov test was used to test for statistical significance between distributions. This test is sensitive to changes in the mean and standard deviation of a distribution.

Picrosirius red staining and image capture

Tissue sections (7 μm thick) were thawed for 15 min and fixed in 2% paraformaldehyde for 20 min. The slides were then incubated in 0.1% Sirius Red in saturated picric acid for 65 min at room temperature. After washing in water, they were placed in 1% Acetic Acid for 30 min. The sections were then dehydrated using ethanol and xylene and mounted in Permount medium (Fisher Scientific, Pittsburgh, PA). To visualize the birefringent collagen, a polarized light microscopy (Zeiss Axioskop, Thornwood, NY) with a SPOT 2e CCD camera was used to capture the images. Exposure time for red color was 0.1 s. All slides were photographed on the same day. The relative collagen content was calculated based on the staining intensity (normalized by the tissue area), and Student's t-test was used to compare them statistically.

CONFLICT OF INTEREST

The authors state no conflict of interest.

ACKNOWLEDGMENTS

We thank the Microscopy & Image Analysis Laboratory at the University of Michigan for training and providing access to cryostat sectioning. We thank the Fisher Laboratory at the University of Michigan for assistance with the Sirius red staining experiment. We also thank The National Institute of Arthritis and Musculoskeletal and Skin Diseases (grant number AR50562) for support.

SUPPLEMENTARY MATERIAL

Supplementary material is linked to the online version of the paper at http://www.nature.com/jid

REFERENCES

Ashcroft GS, Dodsworth J, vanBoxtel E *et al.* (1997) Estrogen accelerates cutaneous wound healing associated with an increase in TGF-beta 1 levels. *Nat Med* 3:1209–15

Ashcroft GS, Greenwell-Wild T, Horan MA *et al.* (1999) Topical estrogen accelerates cutaneous wound healing in aged humans associated with an altered inflammatory response. *Am J Pathol* 155:1137–46

Bolognia JL (1995) Aging skin. *Am J Med* 98:S99–103

Brincat M, Kabalan S, Studd JWW *et al.* (1987) A study of the decrease of skin collagen content, skin thickness, and bone mass in the postmenopausal woman. *Obstet Gynecol* 70:840–5

Brincat M, Moniz CF, Studd JWW (1983) Sex hormones and skin collagen content in postmenopausal women. *Br Med J* 287:1337–8

Brincat M, Moniz CJ, Studd JWW (1985) Long-term effects of the menopause and sex hormones on skin thickness. *Br J Obstet Gynaecol* 92:256–9

Brincat MP (2000) Hormone replacement therapy and the skin. *Maturitas* 35:107–17

Brincat MP, Baron YM, Galea R (2005) Estrogens and the skin. *Climacteric* 8:110–23

Brodsky B, Eikenberry EF, Cassidy K (1980) An unusual collagen periodicity in skin. *Biochimica et Biophysica Acta (BBA)—Protein Structure* 621:162–6

Calvin M, Dyson M, Rymer J *et al.* (1998) The effects of ovarian hormone deficiency on wound contraction in a rat model. *Br J Obstet Gynaecol* 105:223–7

Castelo-Branco C, Duran M, Gonzalez-Merlo J (1993) Skin collagen changes related to age and hormone replacement therapy. *Obstet Gynecol Surv* 48:277–9

Cuttle L, Nataatmadja M, Fraser JF *et al.* (2005) Collagen in the scarless fetal skin wound: detection with piccosirius-polarization. *Wound Repair Regen* 13:198–204.

Danielson KG, Baribault H, Holmes DF *et al.* (1997) Targeted disruption of decorin leads to abnormal collagen fibril morphology and skin fragility. *J Cell Biol* 136:729–43

Dellmann H-D, Eurell JA (1998) *Textbook of veterinary histology*. Lippincott Williams & Wilkins: Philadelphia, pp 303–32

El-Domyati M, Attia S, Saleh F *et al.* (2002) Intrinsic aging vs. photoaging: a comparative histopathological, immunohistochemical, and ultrastructural study of skin. *Exp Dermatol* 11:398–405

Fisher GJ, Quan T, Purohit T *et al.* (2009) Collagen fragmentation promotes oxidative stress and elevates matrix metalloproteinase-1 in fibroblasts in aged human skin. *Am J Pathol* 174:101–14

Fleet MR (2006) Development of black pigmented skin spots and pigmented wool fibres in a Merino flock—Causes, field observations, and wool measurement. *Aust J Agric Res* 57:751–60

Flint MH, Craig AS, Reilly HC *et al.* (1984) Collagen fibril diameters and glycosaminoglycan content of skins—Indices of tissue maturity and function. *Connect Tissue Res* 13:69–81

Forrest JW, Fleet MR (1986) Pigmented spots in the wool-bearing skin on white merino sheep induced by ultraviolet light. *Aust J Biol Sci* 39:125–36

Gathercole LJ, Shah JS, Nave C (1987) Skin-tendon differences in collagen D-period are not geometric or stretch-related artefacts. *Int J Biol Macromol* 9:181–3

Gilchrest BA (1996) A review of skin ageing and its medical therapy. *Br J Dermatol* 135:867–75

Goldsmith LA (1991) *Physiology, biochemistry, and molecular biology of the skin*. Oxford University Press: New York, 2 v. (xxii, 1529 p).

Graham HK, Hodson NW, Hoyland JA *et al.* (2010) Tissue section AFM: *In situ* ultrastructural imaging of native biomolecules. *Matrix Biol* 29:254–60

Gupta HS, Seto J, Krauss S *et al.* (2010) *In situ* multi-level analysis of viscoelastic deformation mechanisms in tendon collagen. *J Struct Biol* 169:183–91

Gupta HS, Zioupos P (2008) Fracture of bone tissue: The 'hows' and the 'whys'. *Med Eng Phys* 30:1209–26

Haczynski J, Tarkowski R, Jarzabek K *et al.* (2002) Human cultured skin fibroblasts express estrogen receptor alpha and beta. *Int J Mol Med* 10:149–53

Hodge AJ, Petruska JA (eds) (1963) *Recent Studies with the Electron Microscope on Ordered Aggregates of the Tropocollagen Molecule*. Academic Press: New York

Junqueira LC, Cossermelli W, Brentanti R (1978) Differential staining of collagen type I, II and III by Sirius Red and polarization microscopy. *Arch Histol Jpn* 41:267–74

Lee KH, Kuczera K, Banaszak Holl MM (2011) The severity of osteogenesis imperfecta: A comparison to the relative free energy differences of collagen model peptides. *Biopolymers* 95:182–93

Les CM, Spence CA, Vance JL *et al.* (2004) Determinants of ovine compact bone viscoelastic properties: Effects of architecture, mineralization, and remodeling. *Bone* 35:729–38

Les CM, Vance JL, Christopherson GT *et al.* (2005) Long-term ovariectomy decreases ovine compact bone viscoelasticity. *J Orth Res* 23:869–76

Markiewicz M, Asano Y, Znoyko S *et al.* (2007) Distinct effects of gonadectomy in male and female mice on collagen fibrillogenesis in the skin. *J Dermatol Sci* 47:217–26

Naylor EC, Watson REB, Sherratt MJ (2011) Molecular aspects of skin ageing. *Maturitas* 69:249–56

Orgel JPRO, Miller A, Irving TC *et al.* (2001) The *in situ* supermolecular structure of type I collagen. *Structure* 9:1061–9

Ozyazgan I, Liman N, Dursun N *et al.* (2002) The effects of ovariectomy on the mechanical properties of skin in rats. *Maturitas* 43:65–74

Pierard GE, Letawe C, Dowlati A *et al.* (1995) Effect of hormone replacement therapy for menopause on the mechanical properteis of skin. *J Am Geriatr Soc* 43:662–5

Pierard GE, Pierard-Franchimont C, Vanderplaetsen S *et al.* (2001) Relationship between bone mass density and tensile strength of the skin in women. *Eur J Clin Invest* 31:731–5

Purslow PP, Wess TJ, Hukins DWL (1998) Collagen orientation and molecular spacing during creep and stress-relaxation in soft connective tissues. *J Exp Biol* 201:135–42

Puxkandl R, Zizak I, Paris O *et al.* (2002) Viscoelastic properties of collagen: synchrotron radiation investigations and structural model. *Philos Trans R Soc Lond B Biol Sci* 357:191–7

Sherratt M (2009) Tissue elasticity and the ageing elastic fibre. *AGE* 31:305–25

Stinson RH, Sweeny PR (1980) Skin collagen has an unusual d-spacing. *Biochimica et Biophysica Acta (BBA)—Protein Structure* 621:158–61

Uitto J (1986) Connective tissue biochemistry of the aging dermis. Age-related alterations in collagen and elastin. *Dermatol Clin* 4:433–46

Verzijl N, DeGroot J, Thorpe SR *et al.* (2000) Effect of collagen turnover on the accumulation of advanced glycation end products. *J Biol Chem* 275:39027–31

Wallace JM, Chen Q, Fang M *et al.* (2010a) Type I collagen exists as a distribution of nanoscale morphologies in teeth, bones, and tendons. *Langmuir* 26:7349–54

Wallace JM, Erickson B, Les CM *et al.* (2010b) Distribution of type I collagen morphologies in bone: Relation to estrogen depletion in bone. *Bone* 46:1349–54

Wallace JM, Orr BG, Marini JC *et al.* (2011) Nanoscale morphology of type I collagen is altered in the Brtl mouse model of *Osteogenesis Imperfecta*. *J Struct Biol* 173:146–52

Waller JM, Maibach HI (2006) Age and skin structure and function, a quantitative approach (II): protein, glycosaminoglycan, water, and lipid content and structure. *Skin Res Technol* 12:145–54

Wenstrup RJ, Florer JB, Brunskill EW *et al.* (2004) Type V collagen controls the initiation of collagen fibril assembly. *J Biol Chem* 279:53331–7

Yeh JT, Yeh LK, Jung SM *et al.* (2010) Impaired skin wound healing in lumican-null mice. *Br J Dermatol* 163:1174–80